

Mechanical behaviour of partially crystallized amorphous alloys

S. TAKAYAMA*, R. MADDIN

Department of Metallurgy and Materials Science, University of Pennsylvania, Philadelphia, Pennsylvania, USA

Deformation and fracture of partially crystallized $\text{Ni}_{55}\text{Pd}_{35}\text{P}_{10}$ amorphous alloys have been investigated. The samples with a few percent crystallization show a fracture stress (175 kg mm^{-2}) and apparent Young's modulus ($19.5 \times 10^3 \text{ kg mm}^{-2}$) greater than those completely amorphous or partially crystallized 50%. On the other hand, the fracture strain of the former are lower than those of the two latter. A simulated model with mixtures of carborundum powder with grease, shows accord with morphological and mechanical aspects of the partially crystallized alloys. As expected, microcrystals embedded in an amorphous material act as obstacles to plastic flow.

1. Introduction

In earlier reports [1-3] of the deformation and fracture of partially crystallized amorphous alloys it was shown that the fracture stresses were often higher than those of the amorphous alloys with associated increased brittleness. A granular fracture morphology was also reported. Consequently, deformation and fracture of partially crystallized $\text{Ni}_{55}\text{Pd}_{35}\text{P}_{10}$ alloys appeared of interest for more detailed study. The application of our simulated flow model, reported elsewhere [4, 5], could also be applied to the fracture morphology of the amorphous-microcrystalline alloys.

2. Experimental procedure

The powder metallurgy method was used to prepare $\text{Ni}_{55}\text{Pd}_{35}\text{P}_{10}$ alloys. Fully amorphous and partially crystallized samples were prepared by a modified Pond and Maddin method [6]. The quenched filaments were examined using X-ray diffraction techniques to determine the extent of the amorphous state. A partially crystallized sample produces a few weak but relatively sharp bands superimposed upon a diffuse broad band characteristic of the amorphous phase. The filaments were thinned in an ion-milling machine and TEM verified the degree of the crystallization [7].

Ribbon filaments, 15 to 50 μm thick and 0.05

to 0.5 mm wide, were cut into 25 mm long specimens for tensile tests. The samples were deformed at room temperature using an Instron mechanical testing machine. Observations of fracture surfaces were carried out in a scanning electron microscope.

3. Results and discussion

Typical stress-strain curves for fully amorphous and partially crystallized alloys (50% and a few percent, respectively) are listed in Table I and shown in Fig. 1. The fracture stress and Young's modulus of the lightly crystallized samples are greater than those crystallized 50%, whereas the fracture strains of the former are lower than those of the latter.

One of the typical fracture surfaces in the 50% partially crystallized alloy is shown in Fig. 2. This fracture surface also consists of two zones, i.e., a featureless part and one showing a characteristic pattern. Applying the same analysis as in the "completely" amorphous case [4, 7], the featureless part results from a shear fracture mode while the other part derives from a shear and tension fracture mode. In contrast to the "completely" amorphous state of this alloy, the fracture is apparently integranular in both regions. Greater detail of this part is shown in Fig. 2b. It appears that the plastic flow was interrupted by some in-

*Present address: Materials Research Center, Allied Chemical Corporation, Morristown, NJ 07960, USA.

TABLE I Mechanical properties of $\text{Ni}_{55}\text{Pd}_{35}\text{P}_{10}$ alloys (strain-rate $5 \times 10^{-4} \text{ sec}^{-1}$): am = amorphous, RT = room temperature, gauge length = 15 mm (average value of five specimens).

| Specimen | Structure | Testing temperature | Hardness | Fracture stress | Fracture strain | Apparent yield stress | Apparent yield strain | Young's modulus |
|---|----------------------|---------------------|----------|-------------------------|-----------------|-------------------------|-----------------------|-------------------------|
| | | (K) | (DPN) | (kg mm^{-2}) | (%) | (kg mm^{-2}) | (%) | (kg mm^{-2}) |
| $\text{Ni}_{55}\text{Pd}_{35}\text{P}_{10}$ | am | RT | 547 | 149 | 1.41 | 118 | 1.060 | 11.0×10^3 |
| | a few % crystal + am | RT | | 175 | 1.06 | 118 | 0.675 | 19.5×10^3 |
| | 50% + am | RT | | 146 | 1.14 | 115 | 0.783 | 14.4×10^3 |

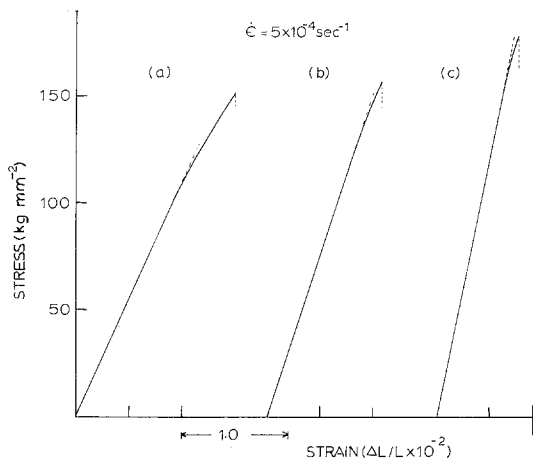


Figure 1 Stress-strain curves of amorphous and partially crystallized $\text{Ni}_{55}\text{Pd}_{35}\text{P}_{10}$ alloys: (a) fully amorphous sample, (b) sample partially crystallized about 50% and (c) sample partially crystallized a few %.

clusions (probably microcrystals embedded in the amorphous state). Fig. 3 shows a transmission electron micrograph of one of the torn fracture parts in the same sample as that of Fig. 2. The many dark spots in the photo show the presence of microcrystals.

Comparing the morphology of this sample with that of the "complete" amorphous state [7], the torn morphology is irregular. Fig. 3 reveals more clearly that these partially crystallized phases act as obstacles to the plastic flow. Therefore, it appears that the crystalline phase affects not only the mechanical properties but also the morphologies on the fracture surfaces. Fig. 4 shows the change in the morphology on the fracture surfaces with increasing crystallization. The degree of the crystallization increases as we proceed from (a) a few %, to (e) 50%. Note that as the degree of crystallization is increased, the smooth fracture surface and ridge patterns disappear and become intergranular. On the other hand, a complete view of the mechanical

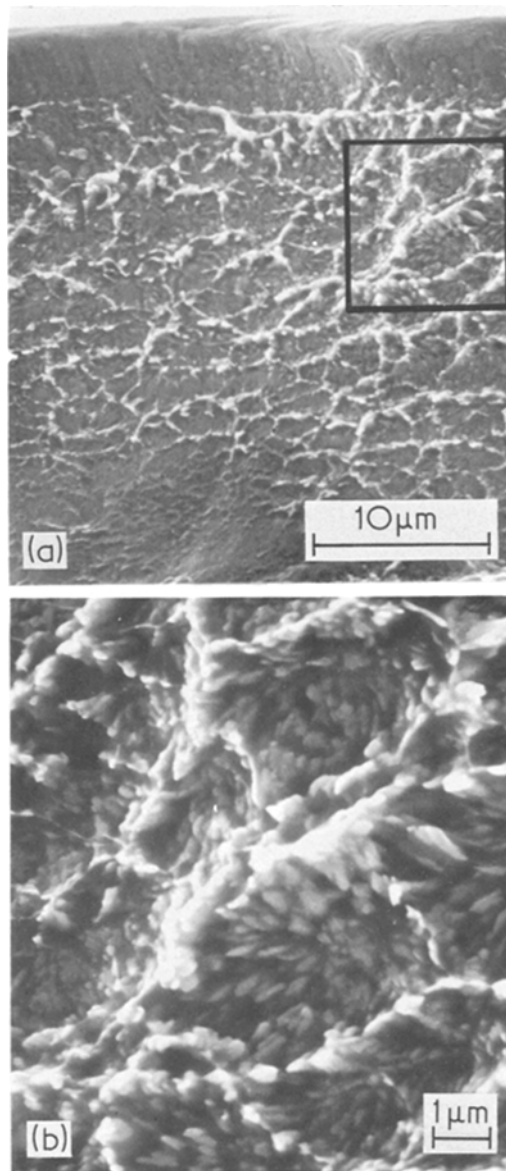


Figure 2 Scanning electron micrographs of the fracture surface typical of 50% crystallized specimens. The outlined areas are magnified in the bottom micrograph.

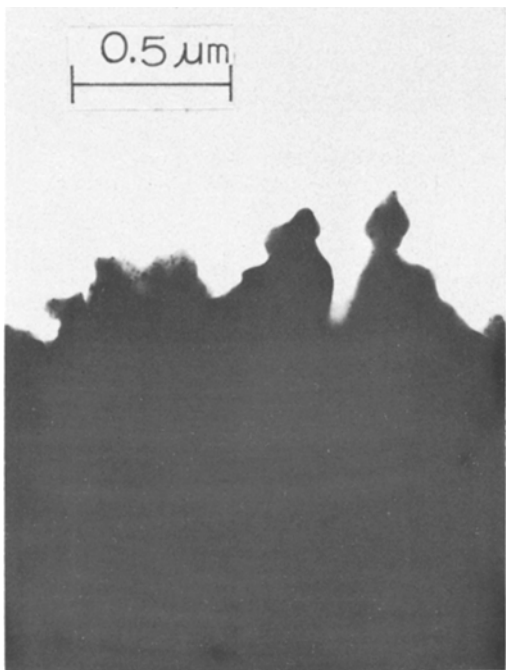


Figure 3 Transmission electron micrograph of the tearing section in a 50% crystallized $\text{Ni}_{55}\text{Pd}_{35}\text{P}_{10}$ alloy.

properties' dependence on crystallization has already been reported in $\text{Pd}_{80}\text{Si}_{20}$ amorphous alloys [1]. It shows that as the metastable phases (MS) appear in the amorphous matrix, the fracture stress goes through a maximum. This tendency is in good agreement with the behaviour of the partially crystalline $\text{Ni}_{55}\text{Pd}_{35}\text{P}_{10}$ alloys (see Table I).

To confirm this microcrystalline phase effect on plastic flow, simulation with the grease model was made by mixing carborundum powder with the grease. After mechanically mixing the carborundum

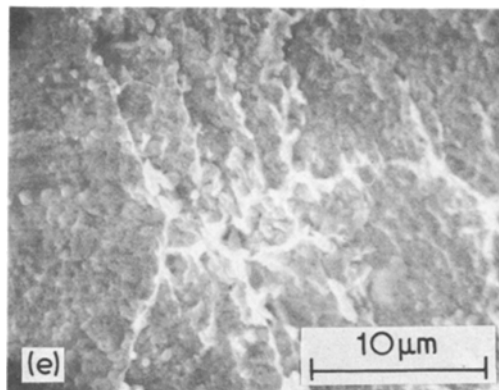
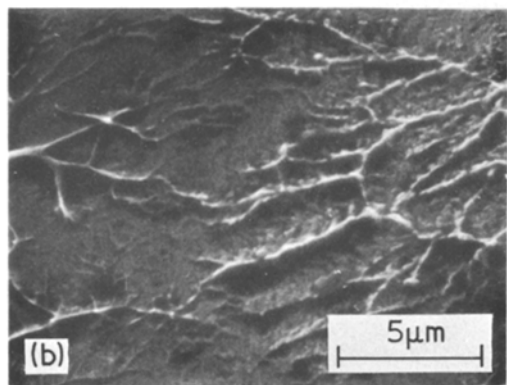
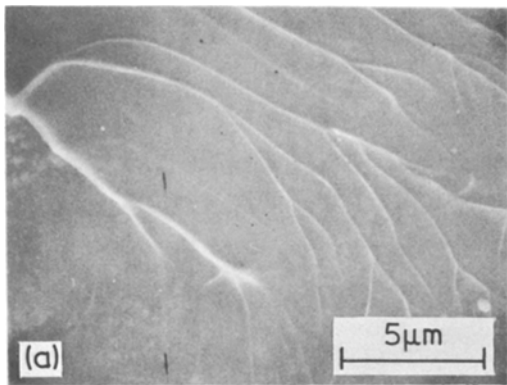
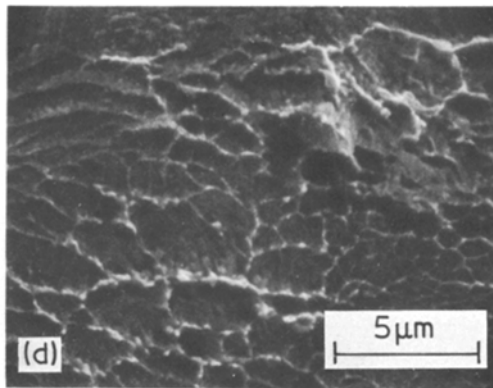
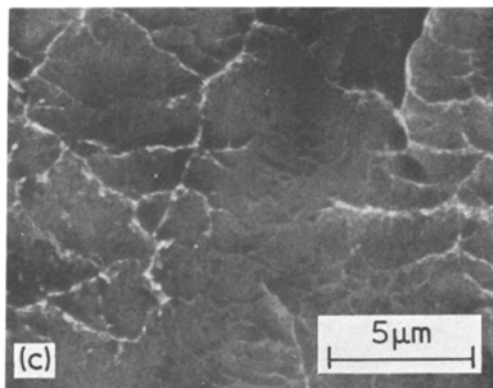


Figure 4 Scanning electron micrograph of the tearing fracture in $\text{Ni}_{55}\text{Pd}_{35}\text{P}_{10}$ partially crystallized alloys: (a) an alloy partially crystallized a few % to (e) 50%.

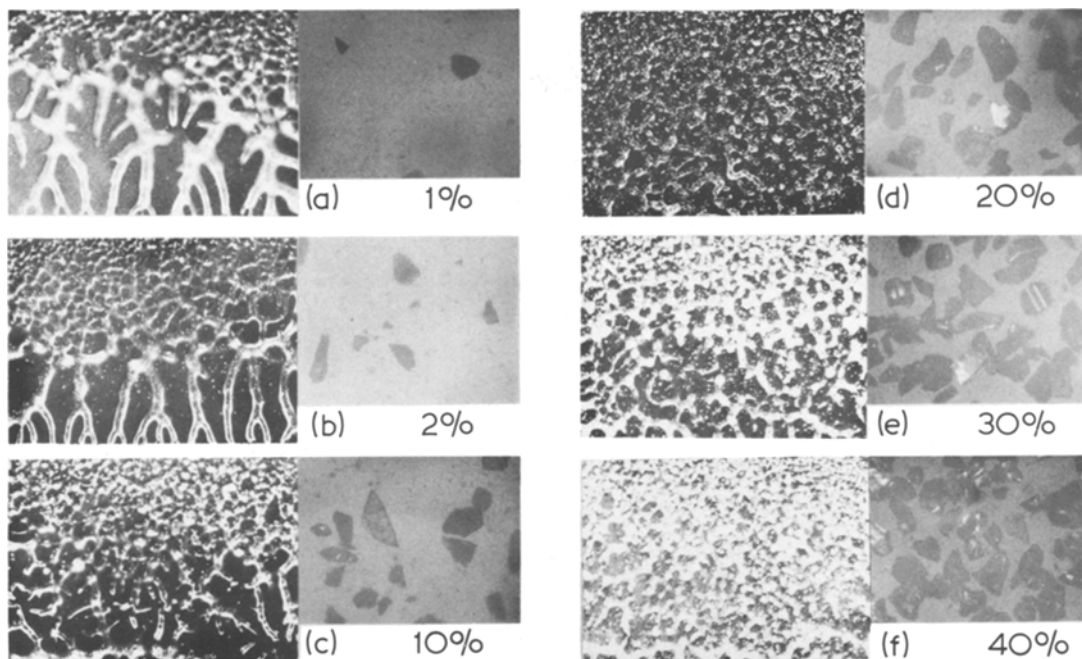


Figure 5 Simulation of the effect of the fracture surfaces by using a grease model as a function of the concentration of carborundum powder. The percentage under each photo denotes the carborundum content. The structure of the mixed grease is shown at the right in an optical micrograph for each case.

powder with the vacuum grease in the desired amount, equal amounts of these prepared greases were carefully weighed and mounted on the same area of glass plate ($25 \times 15 \text{ mm}^2$) and the plates were then sandwiched together. Thereafter, these prepared grease and glass-plate systems were mounted and pulled in an Instron testing machine at the same cross-head speed. Each load needed to separate the glass plates was then recorded on chart paper.

After the separation of the two slides, the patterns produced were photographed. These results are shown in Figs. 5 and 6. As expected, the resultant flow patterns are different with different carborundum concentrations; that is, by increasing the carborundum concentration, the size and the smoothness of the corresponding ridge pattern is reduced as shown in Fig. 5a to f. Obviously, these morphological aspects show the same tendency as for the partially crystalline alloys (compare Fig. 4 with Fig. 5). Moreover, the loads applied in the separation of the two slides in the model first increase and then decrease with increasing carborundum concentration, going through a maximum at a particular concentration, as shown in Fig. 6. Consequently, a small amount of carborundum, corresponding to a slightly crystallized amorphous phase, acts as an obstacle for the viscous flow of the

vacuum grease, increasing the applied load. Since the absorbing force between the grease and the glass will be reduced due to too large a concentration of carborundum particles, the load necessary to separate the two slides will decrease beyond some critical carborundum concentration. We suspect that this situation corresponds to the 50% partially crystallized $\text{Ni}_{55}\text{Pd}_{35}\text{P}_{10}$ alloy. The curve in

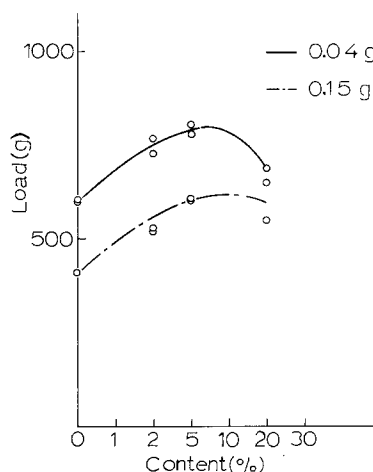


Figure 6 Applied load (g) to produce the simulation fracture patterns versus the carborundum concentration in a vacuum grease. Solid and dash lines show the amount of the vacuum grease mounted on the same area ($25 \times 15 \text{ mm}^2$) of a glass slide, i.e. 0.04 and 0.15 g respectively.

Fig. 6 is in reasonable accord with the fracture stress curve in [1]. Moreover, it is noteworthy (Fig. 6) that the curve of 0.04 g samples is always higher than that of the 0.15 g samples. In other words, the greater the amount of grease content the smaller the force necessary to separate the two slides. Although this behaviour results from the stress condition in the grease between the two slides, it is predictable that as the thickness of a yield or plastic zone during deformation and fracture in a real amorphous state is increased, the fracture stress would decrease. Another important result is that a small amount of a crystalline phase acts as an obstacle to plastic flow within the amorphous matrix resulting in increasing the fracture stress. These results are not only limited to the amorphous alloys, but may well apply to some amorphous polymers [8].

4. Conclusions

(1) The fracture stress and Young's modulus of the lightly crystallized samples are greater than those fully amorphous or crystallized 50%, whereas the fracture strains of the former are lower than the latter two.

(2) The morphological and mechanical aspects of

partially crystallized alloys were reproduced by a simulated flow model. It was shown that microcrystals embedded in an amorphous material act as obstacles to plastic flow.

Acknowledgements

We gratefully acknowledge the valuable comments and advice given by Dr L. A. Davis. This work was supported by the Office of Naval Research and the National Science Foundation.

References

1. T. MASUMOTO and R. MADDIN, *Acta Met.* **19** (1971) 725.
2. H. J. LEAMY, H. S. CHEN and T. T. WANG, *Met. Trans.* **3** (1972) 699.
3. P. CHOU and F. SPAEPEN, *Acta Met.* **23** (1975) 609.
4. S. TAKAYAMA and R. MADDIN, Crystal Growth International Conference, Tokyo (1973).
5. *Idem*, *Phil. Mag.* **32** (1975) 457.
6. R. POND JUN. and R. MADDIN, *Trans. Met. Soc. AIME* **245** (1969) 2475.
7. S. TAKAYAMA, Ph. D. Thesis, University of Pennsylvania (1974).
8. K. E. PALMANTEER and M. J. HUNTER, *J. Appl. Polymer Sci.* **1** (1959) 3.

Received 9 June and accepted 23 June 1975.